

On Combinatorial Properties Of Discrete Planar Surfaces

Yukiko Kenmochi and Atsushi Imiya

Abstract

The simplest free boundary in a 3-dimensional space is a moving plane. For the numerical analyses of such simple free boundary problems, it is necessary to express moving planes in a grid space. A simple example of 3-dimensional grid spaces is a set of 3-dimensional lattice points whose coordinates are all integers. In this paper, therefore, we study geometric and topological properties of planes in such a 3-dimensional integer lattice space.

ON COMBINATORIAL PROPERTIES OF DISCRETE PLANAR SURFACES

YUKIKO KENMOCHI AND ATSUSHI IMIYA

Abstract. The simplest free boundary in a 3-dimensional space is a moving plane. For the numerical analyses of such simple free boundary problems, it is necessary to express moving planes in a grid space. A simple example of 3-dimensional grid spaces is a set of 3-dimensional lattice points whose coordinates are all integers. In this paper, therefore, we study geometric and topological properties of planes in such a 3-dimensional integer lattice space.

1 Introduction

The simplest free boundary in a 3-dimensional space is a moving plane. For the numerical analyses of such simple free boundary problems, it is necessary to express moving planes in a grid space. A simple example of 3-dimensional grid spaces is a set of 3-dimensional lattice points whose coordinates are all integers. In this paper, therefore, we study geometric and topological properties of planes in such a 3-dimensional integer lattice space.

In the context of digital geometry for computer imagery, French research group has proposed the theory of naive planes using algebraic properties of a lattice space and examined the algebraic properties of naive planes [1,2,3,4]. Their treatment of digital objects defined in an integer lattice space is based on the theory of the geometry of numbers, which has the long history from H. Minkowski (1864-1909) [5].

On the other hand, we have proposed a combinatorial approach for expression and extraction of boundaries of digital objects [6]. In this paper, we apply our boundary extraction algorithm for digitization of planes, and construct discrete planar surfaces which are planes in an integer lattice space. Because of the equivalence between our

discrete planar surfaces and naive planes, we derive the combinatorial properties of our discrete planar surfaces from the geometric properties of naive planes.

2 Definition of Discrete Combinatorial Surfaces

In this section, we introduce the definition of surfaces in a 3-dimensional integer lattice space based on the approach of combinatorial topology [7]. Let \mathbf{Z} be the set of all integers; \mathbf{Z}^3 denotes the set of lattice points, whose coordinates are all integers. In \mathbf{Z}^3 we define three different neighborhoods of a lattice point $\mathbf{x} = (i, j, k)$ as follows:

$$\mathbf{N}_m(\mathbf{x}) = \{(p, q, r) \in \mathbf{Z}^3 : (i - p)^2 + (j - q)^2 + (k - r)^2 \leq t\}, \quad (1)$$

where $m = 6, 18, 26$ corresponding to $t = 1, 2, 3$. They are called 6-, 18- and 26-neighborhoods, respectively. Depending on each neighborhood, we define elements of 1-dimensional curves and 2-dimensional surfaces in \mathbf{Z}^3 . These elements are called 1- and 2-dimensional discrete simplexes and abbreviated as 1- and 2-simplexes, respectively. Suppose we define 0-dimensional discrete simplexes, which are called 0-simplexes, as isolated points in \mathbf{Z}^3 . Let \mathbf{R} be the set of real numbers; \mathbf{R}^3 denotes the 3-dimensional Euclidean space. Then 1- and 2-simplexes are defined recursively as follows.

Definition 1 *An n -simplex for $n = 1, 2$ is defined as a set of k points in \mathbf{Z}^3 ,*

$$[\mathbf{x}_1, \mathbf{x}_2, \dots, \mathbf{x}_k] = \{\mathbf{x}_1, \mathbf{x}_2, \dots, \mathbf{x}_k\}, \quad (2)$$

so that the closed convex hull of $\mathbf{x}_1, \mathbf{x}_2, \dots, \mathbf{x}_k$ is one of n -dimensional minimum nonzero regions in \mathbf{R}^3 which are bounded by the closed convex hulls of $(n - 1)$ -simplexes.

According to Definition 1, a 1-simplex is defined as a set of two points in \mathbf{Z}^3 , so that those two points are the endpoints of a line segment which has a minimum nonzero length in \mathbf{R}^3 . In other words, a 1-simplex consists of two neighboring points in \mathbf{Z}^3 . The configurations of those two neighboring points depend on the neighborhood systems. The first line of Table 1 shows that there are one, two and three different 1-simplexes for the 6-, 18- and 26-neighborhood systems, respectively. Similarly, a 2-simplex is defined as a set of points whose closed convex hull is bound by a set of the closed convex hulls of 1-simplexes. In addition, the closed convex hull of a 2-simplex holds a 2-dimensional minimum nonzero area. Consequently, one four-point 2-simplex is defined for the 6-neighborhood system, two three-point and one four-point 2-simplexes are defined for the 18-neighborhood system, and three three-point 2-simplexes are defined for the 26-neighborhood system as shown in the second line of Table 1. Note that the congruent 1- and 2-simplexes that

	N ₆	N ₁₈			N ₂₆		
1D							
2D							

Table 1: 1- and 2-simplexes which are respectively regarded as 1- and 2-dimensional elements in \mathbf{Z}^3 for the 6-, 18- and 26-neighborhood systems. All discrete simplexes in \mathbf{Z}^3 are obtained by rotation and translation of those in the table.

differ from those in Table 1 by rotation and translation are omitted in the table. The constructive definitions of 1- and 2-simplexes are presented in [6].

If an n_1 -simplex is a subset of an n_2 -simplex where $n_1 < n_2$, the n_1 -simplex is called a face of the n_2 -simplex; it is also called an n_1 -face because of the dimension. For instance, a 2-simplex for the 26-neighborhood system has three 0-faces and three 1-faces. A set of all faces included in a discrete simplex $[a] = [\mathbf{x}_1, \mathbf{x}_2, \dots, \mathbf{x}_k]$ is denoted by $face([a])$. Let the closed convex hull of k points, $\mathbf{x}_1, \mathbf{x}_2, \dots, \mathbf{x}_k$, be denoted by $\mathbf{CH}([\mathbf{x}_1, \mathbf{x}_2, \dots, \mathbf{x}_k])$. The embedded discrete simplex is defined as

$$\|a\| = \mathbf{CH}([a]) \setminus \left(\bigcup_{[b] \in face([a])} \mathbf{CH}([b]) \right) \quad (3)$$

for any n -simplex $[a]$. If $[a]$ is an n -simplex, $\|a\|$ is called the embedded n -simplex of $[a]$. An n -simplex and the embedded n -simplex are clearly different since $[a]$ and $\|a\|$ are defined as sets of points in \mathbf{Z}^3 and \mathbf{R}^3 , respectively.

Definition 2 A finite set \mathbf{K} of discrete simplexes is called a discrete complex if the following conditions are satisfied;

1. if $[a] \in \mathbf{K}$, $face([a]) \subseteq \mathbf{K}$;
2. if $[a], [b] \in \mathbf{K}$ and $\|a\| \cap \|b\| \neq \emptyset$, then $[a] = [b]$.

The dimension of \mathbf{K} is equal to the maximum dimension of discrete simplexes which belong to \mathbf{K} . Hereafter, we abbreviate n -dimensional discrete complexes to n -complexes as well as n -simplexes. Suppose that \mathbf{K} is an n -complex. If there exist at least one n -simplex $[a] \in \mathbf{K}$ for every s -simplex $[b] \in \mathbf{K}$ such that $[b] \in face([a])$ and $s < n$, \mathbf{K} is called pure. In addition, if we can find a chain of discrete simplexes between two arbitrary elements $[c], [d] \in \mathbf{K}$, $[c_1] = [c], [c_2], \dots, [c_k] = [d]$, such that $[c_i]$ and $[c_{i+1}]$, $i = 1, 2, \dots, k - 1$, has a common face in \mathbf{K} , \mathbf{K} is called connected.

Definition 3 *If a 2-complex \mathbf{K} is pure and connected, \mathbf{K} is a discrete combinatorial surface.*

More discussion on discrete combinatorial surfaces in the sense of combinatorial topology is given in [6].

3 Construction of Discrete Planar Surfaces

Let \mathbf{X} be a closed subset of \mathbf{R}^3 of the form

$$\mathbf{X} = \{(x, y, z) \in \mathbf{R}^3 : l_1 \leq x \leq l_2, m_1 \leq y \leq m_2, n_1 \leq z \leq n_2\}, \quad (4)$$

where l_i, m_i and n_i are integers for $i = 1, 2$. Let \mathbf{P} be a plane in \mathbf{X} such as

$$\mathbf{P} = \{(x, y, z) \in \mathbf{X} : ax + by + cz + d = 0\}, \quad (5)$$

where a, b, c, d are real numbers. Then the following two regions are separated by \mathbf{P} :

$$\mathbf{H}^- = \{(x, y, z) \in \mathbf{X} : ax + by + cz + d \leq 0\}, \quad (6)$$

$$\mathbf{H}^+ = \{(x, y, z) \in \mathbf{X} : ax + by + cz + d \geq 0\}. \quad (7)$$

Obviously, we have

$$\mathbf{H}^- \cap \mathbf{H}^+ = \mathbf{P}. \quad (8)$$

Now we put

$$\mathbf{Y} = \mathbf{X} \cap \mathbf{Z}^3. \quad (9)$$

From (4),

$$\mathbf{Y} = \{(x, y, z) \in \mathbf{Z}^3 : l_1 \leq x \leq l_2, m_1 \leq y \leq m_2, n_1 \leq z \leq n_2\}. \quad (10)$$

We can consider that \mathbf{Y} is a space of a 3-dimensional digital image whose size is $[l_1, l_2] \times [m_1, m_2] \times [n_1, n_2]$. Just as \mathbf{H}^- and \mathbf{H}^+ in \mathbf{X} , there are two regions in \mathbf{Y} , which are separated by \mathbf{P} as follows:

$$\mathbf{I}^- = \{(x, y, z) \in \mathbf{Y} : ax + by + cz + d \leq 0\}, \quad (11)$$

$$\mathbf{I}^+ = \{(x, y, z) \in \mathbf{Y} : ax + by + cz + d \geq 0\}. \quad (12)$$

We say that \mathbf{I}^- and \mathbf{I}^+ are the digitization of \mathbf{H}^- and \mathbf{H}^+ , respectively. Clearly we have

$$\mathbf{I}^- \cap \mathbf{I}^+ = \mathbf{P} \cap \mathbf{Y}. \quad (13)$$

If there is no lattice point on \mathbf{P} , $\mathbf{P} \cap \mathbf{Y}$ is empty, and hence $\mathbf{I}^- \cap \mathbf{I}^+$ is also empty.

# of black points	configurations of black and white points and an example of P	# of black points	configurations of black and white points and an example of P
1	P1	5	P5
2	P2	6	P6
3	P3	7	P7
4	P4a P4b		

Table 2: Eight possible configurations of black and white points in a $\mathbf{C}_{\mathbf{Y}}(i, j, k)$ such that both black and white points exist in $\mathbf{C}_{\mathbf{Y}}(i, j, k)$. An example of \mathbf{P} is also illustrated for each configuration. Note that we ignore the congruent configurations that differ from those eight configurations by rotation and translation.

For both \mathbf{I}^- and \mathbf{I}^+ , we can construct the boundaries which are discrete combinatorial surfaces with the m -neighborhood system for $m = 6, 18, 26$, denoted by $\partial\mathbf{I}_m^-$ and $\partial\mathbf{I}_m^+$, using the similar algorithm for boundary extraction [6]. Both $\partial\mathbf{I}_m^-$ and $\partial\mathbf{I}_m^+$ are considered to be the digitization of \mathbf{P} and called discrete planar surfaces with respect to \mathbf{P} . In this section, we henceforth present how to generate $\partial\mathbf{I}_m^-$ from \mathbf{I}^- . The same procedure can be applied to generate $\partial\mathbf{I}_m^+$ if \mathbf{I}^- and $\partial\mathbf{I}_m^-$ are replaced by \mathbf{I}^+ and $\partial\mathbf{I}_m^+$, respectively. A discrete combinatorial surface $\partial\mathbf{I}_m^-$ is obtained in the following two stages:

1. for each cubic region of eight points in \mathbf{Y} such as

$$\mathbf{C}_{\mathbf{Y}}(i, j, k) = \{(x, y, z) \in \mathbf{Y} : i \leq x \leq i + 1, j \leq y \leq j + 1, k \leq z \leq k + 1\}, \quad (14)$$

$\partial\mathbf{I}_m^-(i, j, k)$ is obtained as a set of 2-simplexes and their faces by referring to a table;

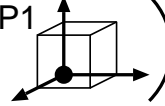
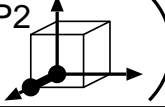
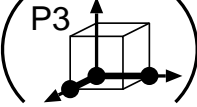
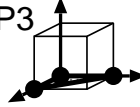
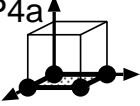
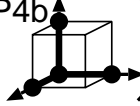
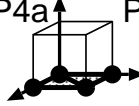
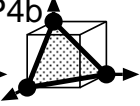
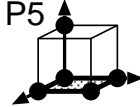



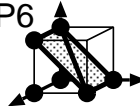


# of black points	N_6	N_{18}	N_{26}
1	(P1 )		
2	(P2 )		
3	(P3 )	P3 	
4	P4a  (P4b )		P4a  P4b 
5	P5 	P5 	P5 
6	P6 	P6 	
7	P7 	P7 	

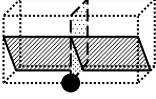
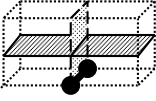
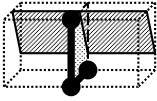
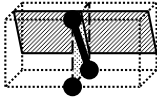
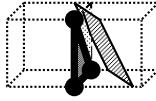
Table 3: A set $\partial\mathbf{I}_m^-(i, j, k)$ for each configuration of black and white points in $\mathbf{C}_\mathbf{Y}(i, j, k)$ corresponding to the configurations in Table 2, $m = 6, 18, 26$. The configurations within parentheses are ignored for the construction of $\partial\mathbf{I}_m^-$ because black points in such $\mathbf{C}_\mathbf{Y}(i, j, k)$ are regarded as 0- or 1-faces of 2-simplexes in the adjacent cubes of $\mathbf{C}_\mathbf{Y}(i, j, k)$.

2. then, we obtain

$$\partial\mathbf{I}_m^- = \bigcup_{(i,j,k) \in \mathbf{Y}} \partial\mathbf{I}_m^-(i, j, k) \quad (15)$$

as a discrete combinatorial surface.

In the first stage, we assign every point in \mathbf{Y} either a black point or a white point. In this case, all points in \mathbf{I}^- and the complement $(\mathbf{I}^-)' = \mathbf{Y} \setminus \mathbf{I}^-$ are assigned black and white points, respectively. In any $\mathbf{C}_\mathbf{Y}(i, j, k)$ such that $\mathbf{C}_\mathbf{Y}(i, j, k) \cap \mathbf{I}^- \neq \emptyset$ and $\mathbf{C}_\mathbf{Y}(i, j, k) \cap (\mathbf{I}^-)' \neq \emptyset$, the black and white points has either of eight different configurations as shown in Table 2, if $0 \leq a \leq b \leq c$ and $c > 0$. For each of these eight configurations, an example of possible \mathbf{P} is also illustrated in Table 2. For each configuration of $\mathbf{C}_\mathbf{Y}(i, j, k)$ in Table 2, $\partial\mathbf{I}_m^-(i, j, k)$ is determined so that all 0-simplexes in $\partial\mathbf{I}_m^-(i, j, k)$ are black points

configuration of black points	N_6	N_{18} and N_{26}	
PJ1			
PJ2			
PJ3			

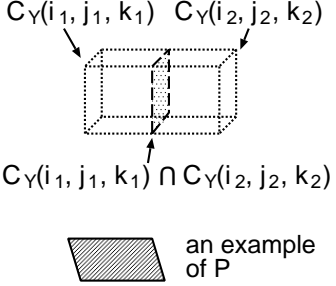


Table 4: The configurations of black points at $\mathbf{C}_Y(i_1, j_1, k_1) \cap \mathbf{C}_Y(i_2, j_2, k_2)$ such that $\mathbf{C}_Y(i_1, j_1, k_1) \cap \mathbf{C}_Y(i_2, j_2, k_2)$ consists of four lattice points. We ignore the congruent configurations that differ from those three configurations by rotation and translation.

and every embedded 2-simplex in $\partial \mathbf{I}_m^-(i, j, k)$ is located as close as possible to \mathbf{P} in \mathbf{X} , as shown in Table 3; for more details of how to generate Table 3, see in [6]. If no 2-simplex exists in $\mathbf{C}_Y(i, j, k)$, we simply set $\partial \mathbf{I}_m^-(i, j, k) = \emptyset$. For instance, configurations P1 and P2 in Table 2 have no 2-simplex since there are only one and two black points in $\mathbf{C}_Y(i, j, k)$, respectively; these black points constitute 0- and 1-faces of 2-simplexes in the adjacent cubes of $\mathbf{C}_Y(i, j, k)$. Similarly, configurations P3 and P4b are ignored for the 6-neighborhood system since black points constitute two and three 1-faces of 2-simplexes in the adjacent cubes of $\mathbf{C}_Y(i, j, k)$, respectively.

In the second stage, we make a union $\partial \mathbf{I}_m^-$ of all $\partial \mathbf{I}_m^-(i, j, k)$ which are obtained by referring to Table 3. In order to prove that $\partial \mathbf{I}_m^-$ is a discrete combinatorial surface, we consider two adjacent unit cubes $\mathbf{C}_Y(i_1, j_1, k_1)$ and $\mathbf{C}_Y(i_2, j_2, k_2)$ such that $\mathbf{C}_Y(i_1, j_1, k_1) \cap \mathbf{C}_Y(i_2, j_2, k_2)$ consists of four lattice points, and $\partial \mathbf{I}_m^-(i_1, j_1, k_1)$ and $\partial \mathbf{I}_m^-(i_2, j_2, k_2)$. Each of four lattice points at $\mathbf{C}_Y(i_1, j_1, k_1) \cap \mathbf{C}_Y(i_2, j_2, k_2)$ is either a black or white point. Table 4 shows that there are three different configurations of black and white points at $\mathbf{C}_Y(i_1, j_1, k_1) \cap \mathbf{C}_Y(i_2, j_2, k_2)$ such that $\mathbf{C}_Y(i_1, j_1, k_1) \cap \mathbf{C}_Y(i_2, j_2, k_2) \cap \mathbf{I}^- \neq \emptyset$. It is also illustrated, in Table 4, that black points at such $\mathbf{C}_Y(i_1, j_1, k_1) \cap \mathbf{C}_Y(i_2, j_2, k_2)$ constitutes the common faces of 2-simplexes of $\partial \mathbf{I}_m^-(i_1, j_1, k_1)$ and $\partial \mathbf{I}_m^-(i_2, j_2, k_2)$. For instance, a black point of configuration PJ1 in Table 4 is a 0-face and a pair of black points of configuration PJ2 is a 1-face. For configuration PJ3, a set of three black points at $\mathbf{C}_Y(i_1, j_1, k_1) \cap \mathbf{C}_Y(i_2, j_2, k_2)$ is regarded differently depending on the neighborhood systems and the location of \mathbf{P} . For the 6-neighborhood system two 1-faces are seen at $\mathbf{C}_Y(i_1, j_1, k_1) \cap \mathbf{C}_Y(i_2, j_2, k_2)$ in PJ3 of Table 4. For the 18- and 26-neighborhood systems either a 1-face or a 2-simplex is seen depending on the location of \mathbf{P} . Thus, given a \mathbf{P}

and an neighborhood system, we can make a union of $\partial\mathbf{I}_m^-(i_1, j_1, k_1)$ and $\partial\mathbf{I}_m^-(i_2, j_2, k_2)$ satisfying the conditions in Definition 2. Therefore, we can obtain $\partial\mathbf{I}_m^-$ as a discrete combinatorial surface, and $\partial\mathbf{I}_m^+$ as well. Since \mathbf{P} is a plane in \mathbf{X} and $\partial\mathbf{I}_m^-$ (resp. $\partial\mathbf{I}_m^+$) is a discrete combinatorial surface as digitization of \mathbf{P} in \mathbf{Y} , $\partial\mathbf{I}_m^-$ (resp. $\partial\mathbf{I}_m^+$) is called a discrete planar surface of \mathbf{P} .

4 Topological Properties of Discrete Planar Surfaces

For $\partial\mathbf{I}_m^-$ and $\partial\mathbf{I}_m^+$, the following proposition is derived from their digitization scheme in section 3; the proof is given in [6].

Proposition 1 *For any plane \mathbf{P} in \mathbf{X} , $\partial\mathbf{I}_m^-$ and $\partial\mathbf{I}_m^+$ are uniquely determined in \mathbf{Y} for each $m = 6, 18, 26$.*

Now, embedding discrete simplexes which are included in $\partial\mathbf{I}_m^-$ and $\partial\mathbf{I}_m^+$ into \mathbf{X} , we respectively obtain

$$\mathbf{P}_m^- = \bigcup_{[a] \in \partial\mathbf{I}_m^-} \|a\| \quad (16)$$

and

$$\mathbf{P}_m^+ = \bigcup_{[a] \in \partial\mathbf{I}_m^+} \|a\| . \quad (17)$$

For any set \mathbf{A} , we denote by \mathbf{A}' the complement of \mathbf{A} and by $\overline{\mathbf{A}}$ the closure of \mathbf{A} . Then, just as \mathbf{H}^- and \mathbf{H}^+ are determined by \mathbf{P} , two regions \mathbf{H}_m^- and \mathbf{H}_m^+ in \mathbf{X} are determined by \mathbf{P}_m^- and \mathbf{P}_m^+ , respectively, such that

$$\mathbf{H}_m^- \subseteq \mathbf{H}^- , \quad (18)$$

$$\mathbf{H}_m^+ \subseteq \mathbf{H}^+ , \quad (19)$$

$$\mathbf{H}_m^- \cap \overline{(\mathbf{H}_m^-)'} = \mathbf{P}_m^- , \quad (20)$$

$$\mathbf{H}_m^+ \cap \overline{(\mathbf{H}_m^+)'} = \mathbf{P}_m^+ \quad (21)$$

for each $m = 6, 18, 26$. Figure 1 illustrates the relation between \mathbf{H}^- and \mathbf{H}^+ and that between \mathbf{H}_m^- and \mathbf{H}_m^+ . The following proposition gives the relations between a triplet of \mathbf{H}_m^- (resp. \mathbf{H}_m^+), $m = 6, 18, 26$, and \mathbf{H}^- (resp. \mathbf{H}^+); the proof is given in [6].

Proposition 2 *For any plane \mathbf{P} , the inclusion relations*

$$\mathbf{H}_6^- \subseteq \mathbf{H}_{18}^- \subseteq \mathbf{H}_{26}^- \subseteq \mathbf{H}^- \quad (22)$$

and

$$\mathbf{H}_6^+ \subseteq \mathbf{H}_{18}^+ \subseteq \mathbf{H}_{26}^+ \subseteq \mathbf{H}^+ \quad (23)$$

hold.

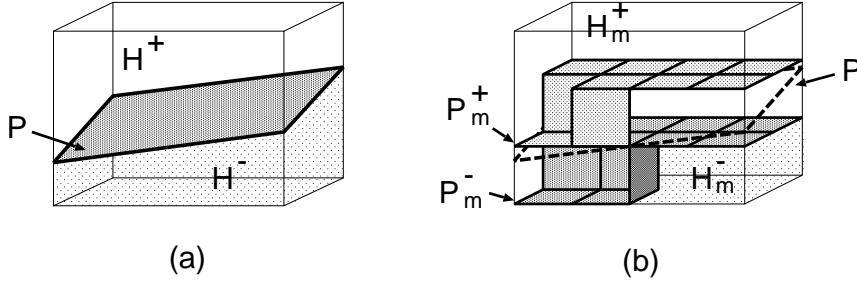


Figure 1: The relation between \mathbf{H}^- and \mathbf{H}^+ in \mathbf{X} (a), and the relation of \mathbf{H}_m^- and \mathbf{H}_m^+ in \mathbf{X} (b). In the figure (b), we assume $m = 6$.

According to Table 3, \mathbf{H}_{18}^- and \mathbf{H}_{26}^- (resp. \mathbf{H}_{18}^+ and \mathbf{H}_{26}^+) are different only if configuration P5 appears in \mathbf{Y} . In other words, \mathbf{H}_{18}^- and \mathbf{H}_{26}^- (resp. \mathbf{H}_{18}^+ and \mathbf{H}_{26}^+) are nearly equivalent; if configuration P5 does not appear in the digitization process of \mathbf{P} , then \mathbf{H}_{18}^- and \mathbf{H}_{26}^- (resp. \mathbf{H}_{18}^+ and \mathbf{H}_{26}^+) are completely equivalent. From Proposition 2, we see that $\partial\mathbf{I}_{26}^-$ is the outermost boundary of \mathbf{I}^- in \mathbf{Y} and \mathbf{P}_{26}^- is the closest to \mathbf{P} in \mathbf{X} .

Let \mathbf{B}_m^- and \mathbf{B}_m^+ be the sets of all lattice points included in $\partial\mathbf{I}_m^-$ and $\partial\mathbf{I}_m^+$ for $m = 6, 18, 26$, respectively, such that

$$\mathbf{B}_m^- = \bigcup_{[a] \in \partial\mathbf{I}_m^-} [a] \quad (24)$$

and

$$\mathbf{B}_m^+ = \bigcup_{[a] \in \partial\mathbf{I}_m^+} [a]. \quad (25)$$

Then, the following theorem is derived.

Theorem 1 *For any plane \mathbf{P} , the inclusion and equality relations*

$$\mathbf{B}_6^- \supseteq \mathbf{B}_{18}^- = \mathbf{B}_{26}^- \quad (26)$$

and

$$\mathbf{B}_6^+ \supseteq \mathbf{B}_{18}^+ = \mathbf{B}_{26}^+ \quad (27)$$

hold.

Proof. Using $\mathbf{C}_\mathbf{Y}(i, j, k)$ of (14), for each m , we define

$$\mathbf{B}_m^-(i, j, k) = \mathbf{B}_m^- \cap \mathbf{C}_\mathbf{Y}(i, j, k) \quad (28)$$

which is a subset of \mathbf{B}_m^- . Let us compare a triplet of $\mathbf{B}_m^-(i, j, k)$, $m = 6, 18, 26$ for every $\mathbf{C}_\mathbf{Y}(i, j, k)$ in \mathbf{Y} . If we make a comparison between $\mathbf{B}_6^-(i, j, k)$ and $\mathbf{B}_{18}^-(i, j, k)$ in Table 3, we see

$$\mathbf{B}_6^-(i, j, k) \supseteq \mathbf{B}_{18}^-(i, j, k) \quad (29)$$

for configurations P4b, P5, P6 and P7, otherwise we obtain

$$\mathbf{B}_6^-(i, j, k) = \mathbf{B}_{18}^-(i, j, k). \quad (30)$$

Between $\mathbf{B}_{18}^-(i, j, k)$ and $\mathbf{B}_{26}^-(i, j, k)$, we see that there is no difference for any configuration in Table 3; even if $\partial\mathbf{I}_{18}^-(i, j, k)$ and $\partial\mathbf{I}_{26}^-(i, j, k)$ are different for P5, $\mathbf{B}_{18}^-(i, j, k) = \mathbf{B}_{26}^-(i, j, k)$. Thus, we obtain

$$\mathbf{B}_{18}^-(i, j, k) = \mathbf{B}_{26}^-(i, j, k) \quad (31)$$

for any $(i, j, k) \in \mathbf{Y}$. From (29), (30) and (31), we see that (26) always hold. Similarly, (27) is also derived. \square

5 Naive Planes as Discrete Planar Surfaces

The naive plane [1] is defined with respect to \mathbf{P} of (5) by

$$\mathbf{NP} = \{(x, y, z) \in \mathbf{Z}^3 : 0 \leq ax + by + cz + d < \omega\} \quad (32)$$

where $\omega = \max\{|a|, |b|, |c|\}$. The properties of local configurations of points in \mathbf{NP} have been already obtained in [1,2,3,4]. In this section, we first show the equivalence between \mathbf{NP} and \mathbf{B}_{26}^+ , and derive combinatorial properties of discrete simplexes in $\partial\mathbf{I}_{26}^+$ from the properties of \mathbf{NP} . In order to prove the next theorem, we refer to Lemma 1 in Appendix A.

Theorem 2 *For any \mathbf{P} ,*

$$\mathbf{NP} = \mathbf{B}_{26}^+ \quad (33)$$

holds.

Proof. Let us consider \mathbf{P} such that $0 \leq a \leq b \leq c$, $c > 0$. In this case $\omega = c$. From (32) we obtain

$$\mathbf{NP} = \{(x, y, z) \in \mathbf{Z}^3 : -\frac{a}{c}x - \frac{b}{c}y - \frac{d}{c} \leq z < -\frac{a}{c}x - \frac{b}{c}y - \frac{d}{c} + 1\}. \quad (34)$$

For every point $\mathbf{x} = (x, y, z)$ in \mathbf{NP} , if we define a point $\mathbf{c} \in \mathbf{P}$ such that

$$\mathbf{c} = (x, y, -\frac{a}{c}x - \frac{b}{c}y - \frac{d}{c}), \quad (35)$$

then we see that

$$0 \leq |\mathbf{x} - \mathbf{c}| < 1 \quad (36)$$

from (34). Thus, to prove this theorem, we will show that every $\mathbf{x} \in \mathbf{B}_{26}^+$ satisfies (36). Let us consider a cubic region $\mathbf{C}_{\mathbf{Y}}(i, j, k)$ of (14). Table 2 gives all configurations of points in \mathbf{I}^- and $(\mathbf{I}^-)'$ for a $\mathbf{C}_{\mathbf{Y}}(i, j, k)$. Since we focus on \mathbf{B}_{26}^+ instead of \mathbf{B}_{26}^- in the theorem, we need to consider that black and white points in Table 2 are points in \mathbf{I}^+ and $(\mathbf{I}^+)'$ instead of \mathbf{I}^- and $(\mathbf{I}^-)'$, respectively. Any black point \mathbf{x} in Table 2 which satisfies (36) is colored black or gray in Table 5; black points in Table 2 which do not satisfy (36) are colored white in Table 5. All black points in Table 5 apparently satisfy (36). For each gray point $\mathbf{g} = (s, t, u)$, if we consider two points in \mathbf{P} such as

$$\mathbf{bg} = (s, -\frac{a}{b}s - \frac{c}{b}u - \frac{d}{b}, u) \quad (37)$$

and

$$\mathbf{cg} = (s, t, -\frac{a}{c}s - \frac{b}{c}t - \frac{d}{c}), \quad (38)$$

we obtain

$$|\mathbf{g} - \mathbf{bg}| \geq |\mathbf{g} - \mathbf{cg}| \quad (39)$$

since $|\mathbf{g} - \mathbf{bg}| : |\mathbf{g} - \mathbf{cg}| = 1/b : 1/c$ from Lemma 1 and $0 < b \leq c$. Let us consider $\mathbf{C}_{\mathbf{Y}}(i, j, k+1)$ such that at least one gray point \mathbf{g} exists in $\mathbf{C}_{\mathbf{Y}}(i, j, k+1)$. If the configuration of $\mathbf{C}_{\mathbf{Y}}(i, j, k)$ is P4b or P5 in Table 5, then the configuration of $\mathbf{C}_{\mathbf{Y}}(i, j, k+1)$ will be P1. Similarly, if the configuration of $\mathbf{C}_{\mathbf{Y}}(i, j, k)$ is P6, the configuration of $\mathbf{C}_{\mathbf{Y}}(i, j, k+1)$ will be P2. We then see that all \mathbf{g} satisfy (36). Since white points in Table 5 do not satisfy (36) obviously, from a comparison between a set of black and gray points in Table 5 and a set of points of \mathbf{B}_{26}^+ in Table 3, we have (33). \square

If we define a naive plane such that

$$\mathbf{NP}^- = \{(x, y, z) \in \mathbf{Z}^3 : -\omega < ax + by + cz + d \leq 0\} \quad (40)$$

instead of \mathbf{NP} , then the following corollary is derived.

Corollary 1 *For any \mathbf{P} ,*

$$\mathbf{NP}^- = \mathbf{B}_{26}^- \quad (41)$$

holds.

In the rest of this section, we discuss the local configurations of discrete simplexes in $\partial\mathbf{I}_{26}^+$ (resp. $\partial\mathbf{I}_{26}^-$). First, the following proposition is automatically derived from the definition of $\partial\mathbf{I}_{26}^+$ (resp. $\partial\mathbf{I}_{26}^-$).

Proposition 3 *Any 2-simplex included in $\partial\mathbf{I}_{26}^+$ (resp. $\partial\mathbf{I}_{26}^-$) is classified into either of three types illustrated in Table 1.*

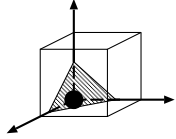
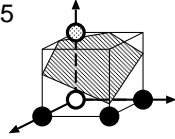
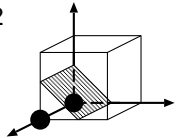
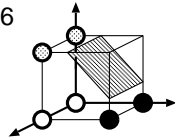
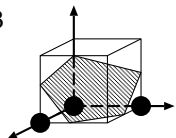
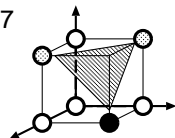
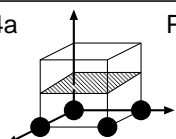
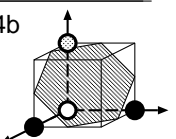
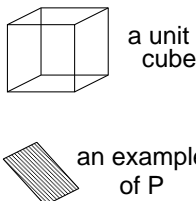
# of points in I^+	configuration of points in I^+ and an example of P	# of points in I^+	configuration of points in I^+ and an example of P
1	P1 	5	P5 
2	P2 	6	P6 
3	P3 	7	P7 
4	P4a  P4b 		 <ul style="list-style-type: none"> \bullet \odot points in B_{26}^+ \circ points in I^+ but not in B_{26}^+

Table 5: The classification of all points in I^+ into two types with respect to each configuration of Table 2: points of B_{26}^+ and other.

From Theorem 2 and the properties of \mathbf{NP} [1,2,3,4], we can derive the following combinatorial properties of ∂I_{26}^+ (resp. ∂I_{26}^-) which are summarized in Propositions 4 to 8. Let us consider the configurations of discrete simplexes in the parts of ∂I_{26}^+ (resp. ∂I_{26}^-) which project on the coordinate plane $z = 0$ as a rectangle whose sizes are $\lambda \times \mu$.

Proposition 4 *In the case of $\lambda = \mu = 2$, there exist five different configurations of discrete simplexes as shown in Figure 2 for ∂I_{26}^+ (resp. ∂I_{26}^-) with respect to any \mathbf{P} such that $0 \leq a \leq b \leq c$, $c > 0$.*

Proposition 5 *At most four different configurations of discrete simplexes for $\lambda = \mu = 2$ are contained in a ∂I_{26}^+ (resp. ∂I_{26}^-).*

Proposition 6 *In the case of $\lambda = \mu = 3$, there exist 40 different configurations of discrete simplexes as shown in Figure 3 for ∂I_{26}^+ (resp. ∂I_{26}^-) with respect to any \mathbf{P} such that $0 \leq a \leq b \leq c$, $c > 0$.*

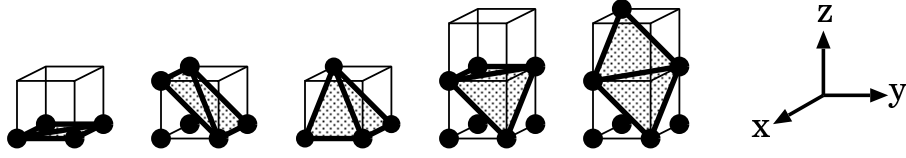


Figure 2: All five configurations of discrete simplexes in $\partial\mathbf{I}_{26}^+$ (resp. $\partial\mathbf{I}_{26}^-$) whose projections on plane $z = 0$ lie on the 2×2 square grids.

Proposition 7 *At most nine different configurations of discrete simplexes for $\lambda = \mu = 3$ are contained in a $\partial\mathbf{I}_{26}^+$ (resp. $\partial\mathbf{I}_{26}^-$).*

Propositions 4 and 5 give the coexistence of two adjacent 2-simplexes in a $\partial\mathbf{I}_{26}^+$ (resp. $\partial\mathbf{I}_{26}^-$). For each 0-simplex $[\mathbf{x}] \in \partial\mathbf{I}_{26}^+$ or $\partial\mathbf{I}_{26}^-$, we can define the star such that

$$\sigma([\mathbf{x}] : \partial\mathbf{I}_{26}^+) = \{[a] \in \partial\mathbf{I}_{26}^+ : [\mathbf{x}] \in \text{face}([a])\} \quad (42)$$

or

$$\sigma([\mathbf{x}] : \partial\mathbf{I}_{26}^-) = \{[a] \in \partial\mathbf{I}_{26}^- : [\mathbf{x}] \in \text{face}([a])\} . \quad (43)$$

The projection of $\sigma([\mathbf{x}] : \partial\mathbf{I}_{26}^+)$ (resp. $\sigma([\mathbf{x}] : \partial\mathbf{I}_{26}^-)$) on the coordinate plane $z = 0$ is in a square whose size is 3×3 if $0 \leq a \leq b \leq c$ and $c > 0$. From this fact, we also derive the following proposition.

Proposition 8 *Any $\partial\mathbf{I}_{26}^+$ (resp. $\partial\mathbf{I}_{26}^-$) is a discrete combinatorial surface with the boundary which consists of 2-simplexes and their faces, such that every 0-simplex $[\mathbf{x}] \in \partial\mathbf{I}_{26}^+$ (resp. $\partial\mathbf{I}_{26}^-$) has one of the stars whose configurations are illustrated in Figure 3 for $\mathbf{x} = (x, y, z)$ where $l_1 < x < l_2$, $m_1 < y < m_2$, $n_1 < z < n_2$.*

We see that the equivalent simplicial configurations of a star can appear in different simplicial configurations each of which projects on the coordinate plane $z = 0$ as a 3×3 square in Figure 3. Thus, the total number of different configurations of discrete simplexes of a star will be less than 40.

Finally, we examine the configurations of discrete simplexes in a $\partial\mathbf{I}_{26}^+$ (resp. $\partial\mathbf{I}_{26}^-$). Let us consider \mathbf{P} of (5) which has the coefficients such that a , b and c are all positive integers and $\mathbf{P} \cap \mathbf{Y} \neq \emptyset$. Let L be the least common multiple of a , b and c , and

$$A = \frac{L}{a} , \quad (44)$$

$$B = \frac{L}{b} \quad (45)$$

and

$$C = \frac{L}{c} . \quad (46)$$

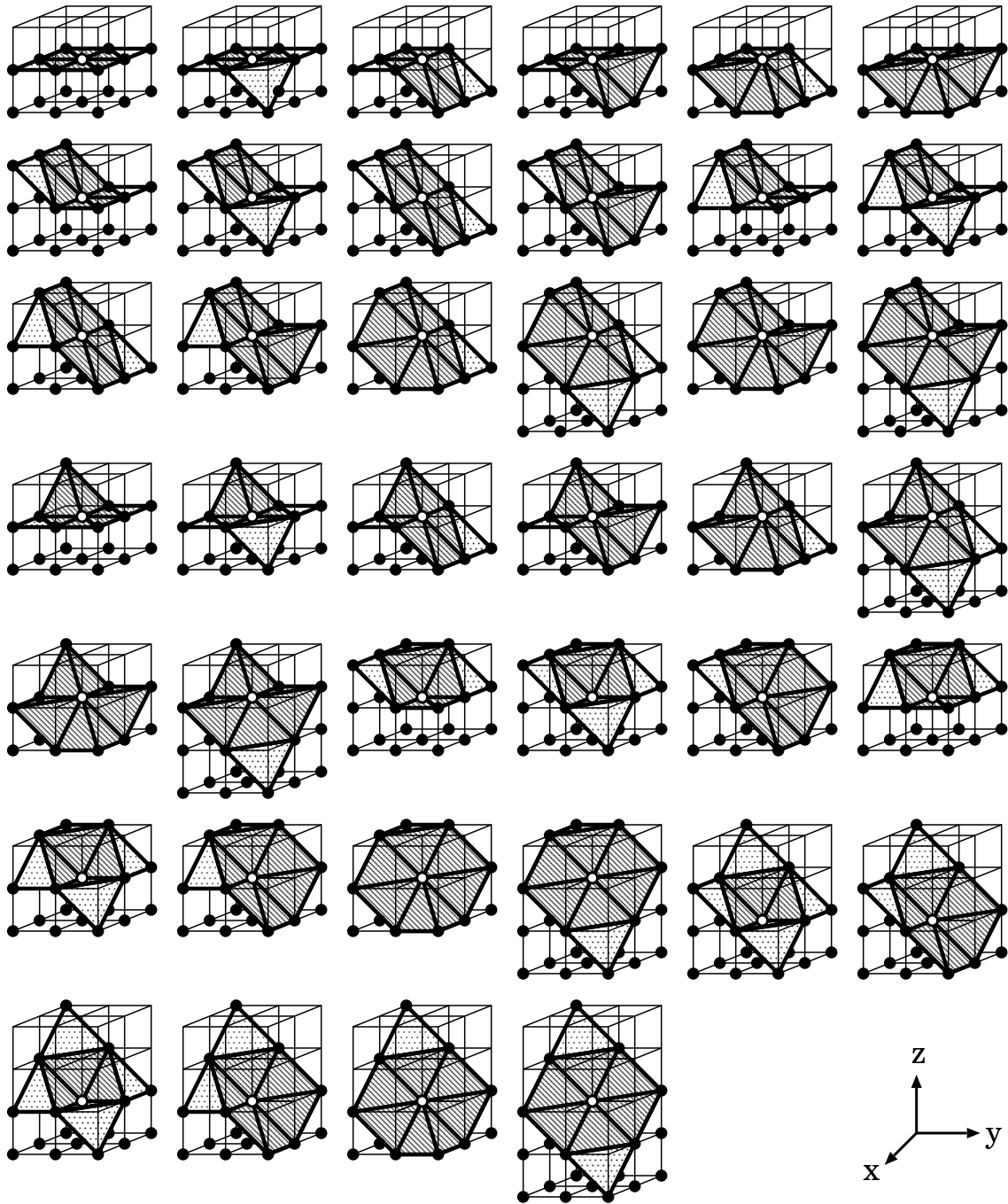


Figure 3: All 40 configurations of discrete simplexes in $\partial\mathbf{I}_{26}^+$ (resp. $\partial\mathbf{I}_{26}^-$) whose projections on plane $z = 0$ lie on the 3×3 square grids. The star of each white point is also shown as discrete simplexes with diagonal lines in the figure.

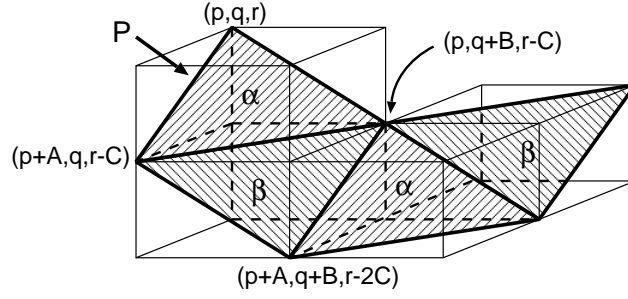


Figure 4: If a lattice point $(p, q, r) \in \mathbf{P} \cap \mathbf{Y}$ exists, a plane \mathbf{P} such that a, b and c are positive integers can be decomposed into two types of the triangles α and β .

Theorem 3 For any \mathbf{P} such that a, b and c are positive integers and there exist $(p, q, r) \in \mathbf{P} \cap \mathbf{Y}$, $\partial\mathbf{I}_{26}^+$ (resp. $\partial\mathbf{I}_{26}^-$) is decomposed into triangular pieces of discrete combinatorial surfaces, which are classified into two types.

Proof. From Lemma 1 in Appendix A, we obtain (51) as illustrated in Figure 5 and then we have

$$\frac{1}{a} : \frac{1}{b} : \frac{1}{c} = A : B : C \quad (47)$$

from (44), (45) and (46). Since A, B and C are relative primes, there is no triangular piece on \mathbf{P} whose vertices are all in \mathbf{Z}^3 and which is smaller than the triangle of type α or β ;

- type α : a triangle whose vertices are (p, q, r) , $(p + A, q, r - C)$ and $(p, q + B, r - C)$;
- type β : a triangle whose vertices are $(p + A, q, r - C)$, $(p, q + B, r - C)$ and $(p + A, q + B, r - 2C)$.

In Figure 4 we see that \mathbf{P} is decomposed into two types of triangles α and β . For each triangular region of \mathbf{P} , we can uniquely obtain a discrete planar surface from Proposition 1. \square

6 Conclusions

This paper is devoted for the study of topological and geometric properties of $\partial\mathbf{I}_{26}^-$ and $\partial\mathbf{I}_{26}^+$. Since we constructed discrete planar surfaces from a set of lattice points, we described the combinatorial properties by using the configurations of discrete simplexes instead of those of lattice points. In this paper, we have proven the equivalence between \mathbf{B}_{26}^+ (resp. \mathbf{B}_{26}^-) and \mathbf{NP} (resp. \mathbf{NP}^-) which are defined by using algebraic approach. From the equivalence, we obtained the combinatorial properties of $\partial\mathbf{I}_{26}^-$ (resp. $\partial\mathbf{I}_{26}^+$), such as the coexistence of adjacent 2-simplexes and the configuration of discrete simplexes of

a star in a $\partial\mathbf{I}_{26}^+$ (resp. $\partial\mathbf{I}_{26}^-$). Similar results for $\partial\mathbf{I}_{18}^+$ and $\partial\mathbf{I}_6^+$ (resp. $\partial\mathbf{I}_{18}^-$ and $\partial\mathbf{I}_6^-$) are in preparation.

Acknowledgments

The first author expresses much thanks for the thoughtful comments of Professor Dr. Reinhard Klette at CITR, the university of Auckland. This work was done during her staying in Auckland, which was supported by Yazaki Memorial Foundation for Science & Technology and the JAIST Foundation.

References

1. J. P. Reveillès, “Combinatorial Pieces in Digital Lines and Planes,” in Proceedings of SPIE, Vol. 2573; Vision Geometry III, pp. 23–34, Spie, 1995.
2. J. Françon, “Sur la topologie d’un plan arithmétique,” Theoretical Computer Science, Vol. 156, pp. 159–176, 1996.
3. J. Françon, J. M. Schramm and M. Tajine, “Recognizing arithmetic straight lines and planes,” in LNCS 1176; Discrete Geometry for Computer Imagery, S. Miguët, A. Montanvert and S. Ubéda(Eds.), pp. 141–150, Springer-Verlag, Berlin, Heidelberg, 1996.
4. I. Debled-Renesson, *Etude et reconnaissance des droites et plans discrets*, PhD thesis, University of Louis Pasteur, 1995.
5. H. Minkowski, *Geometrie der Zahlen*, Leipzig, 1896.
6. Y. Kenmochi, *Discrete Combinatorial Polyhedra: Theory and Application*, Doctoral thesis, Chiba University, 1998.
7. P. S. Aleksandrov, *Combinatorial Topology*, volume 1. Graylock Press, Rochester, New York, 1956.

A Lemma 1

Let us consider \mathbf{P} of (5) such that $a, b, c > 0$. For each point $\mathbf{p} \in \mathbf{I}^+ \setminus \mathbf{P}$ such that $\mathbf{p} = (s, t, u)$, we set three planes such as

$$\mathbf{S} = \{(x, y, z) \in \mathbf{R}^3 : x = s\}, \quad (48)$$

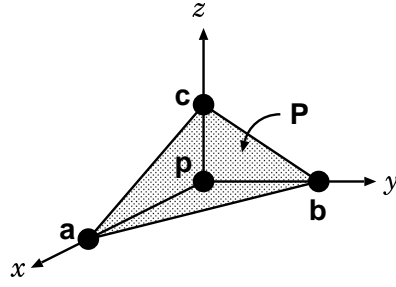


Figure 5: Three points \mathbf{a} , \mathbf{b} and \mathbf{c} defined for a plane \mathbf{P} and a point \mathbf{p} which is not in \mathbf{P} .

$$\mathbf{T} = \{(x, y, z) \in \mathbf{R}^3 : y = t\} \quad (49)$$

and

$$\mathbf{U} = \{(x, y, z) \in \mathbf{R}^3 : z = u\}. \quad (50)$$

Let \mathbf{a} , \mathbf{b} and \mathbf{c} be the intersection points of \mathbf{P} , \mathbf{T} and \mathbf{U} , \mathbf{P} , \mathbf{S} and \mathbf{U} , and \mathbf{P} , \mathbf{S} and \mathbf{T} , respectively, as illustrated in Figure 5. Then the next lemma is derived.

Lemma 1 For any $\mathbf{p} \in \mathbf{I}^+ \setminus \mathbf{P}$, we obtain

$$|\mathbf{p} - \mathbf{a}| : |\mathbf{p} - \mathbf{b}| : |\mathbf{p} - \mathbf{c}| = \frac{1}{a} : \frac{1}{b} : \frac{1}{c} \quad (51)$$

where $a, b, c > 0$.

Proof. The equation of the line which is the intersection of \mathbf{P} and \mathbf{U} is given by

$$ax + by + cu + d = 0. \quad (52)$$

Thus, the slope of the line in \mathbf{U} is given by

$$\frac{|\mathbf{p} - \mathbf{b}|}{|\mathbf{p} - \mathbf{a}|} = \frac{a}{b}. \quad (53)$$

Similarly, the slopes of the intersection lines between \mathbf{P} and \mathbf{T} , and \mathbf{P} and \mathbf{S} , are respectively given by

$$\frac{|\mathbf{p} - \mathbf{c}|}{|\mathbf{p} - \mathbf{b}|} = \frac{b}{c} \quad (54)$$

and

$$\frac{|\mathbf{p} - \mathbf{a}|}{|\mathbf{p} - \mathbf{c}|} = \frac{c}{a}. \quad (55)$$

Thus, we obtain (51). \square

Yukiko Kenmochi
School of Information Science
Japan Advanced Institute of Science and Technology
1-1 Asahidai Tatsunokuchi, Ishikawa 923-1292 Japan
E-mail: kenmochi@jaist.ac.jp

Atsushi Imiya
Department of Information and Image Sciences
Chiba University
1-33 Yayoi-cho Inage-ku, Chiba 263-8522 Japan
E-mail: imiya@ics.tj.chiba-u.ac.jp